Inorganic Chemistry

Article

pubs.acs.org/IC

Disklike Hepta- and Tridecanuclear Cobalt Clusters. Synthesis, Structures, Magnetic Properties, and DFT Calculations

Ji-Dong Leng,[†] Su-Kun Xing,[†,‡] Radovan Herchel,*[,§] Jun-Liang Liu,[†] and Ming-Liang Tong*[,†]

[†]Key Laboratory of Bioinorganic and Synthetic Chemistry of Ministry of Education, State Key Laboratory of Optoelectronic Materials and Technologies, School of Chemistry and Chemical Engineering, Sun Yat-Sen University, Guangzhou 510275, P. R. China

[‡]Beihai Marine Environmental Monitoring Center Station of State Oceanic Administration, Beihai 536000, P. R. China

[§]Department of Inorganic Chemistry, Faculty of Science, Palacky University, 17. listopadu 12, 771 46 Olomouc, Czech Republic

Supporting Information

ABSTRACT: The synthesis, structure and magnetic properties are reported of two disklike mixed-valence cobalt clusters $[Co^{III}Co^{II}_6(thmp)_2(acac)_6(ada)_3]$ (**1**) and $[Co^{III}_2Co^{II}_{11}(thmp)_4(Me_3CCOO)_4(acac)_6(OH)_4(H_2O)_4](Me_3CCOO)_2\cdot H_2O$ (**2**). Heptanuclear complex **1** was prepared by solvothermal reaction of cobalt(II) acetylacetonate ($Co(acac)_2$), 1,1,1-tris(hydroxymethyl)-propane (H_3thmp), and adamantane-1-carboxylic acid (Hada), whereas by substituting Hada with Me_3CCO_2H, tridecanuclear complex **2** was obtained with an unexpected $[Co^{III}_2Co^{II}_{11}]$ core. The core structures of **1** and **2** are related to each other: that of **1** arranges as a centered hexagon of a central Co^{III} ion surrounded by a $[Co^{II}_6]$ hexagon, while that of **2** can be described as a larger oligomer based on two vertex-sharing $[Co^{III}Co^{II}_6]$ clusters. Variable-temperature direct-current magnetic susceptibility measurements demonstrated overall ferromagnetic coupling between the Co^{II} ions within both clusters. The magnetic exchange (J) and magnetic anisotropy (D) values were quantified with appropriate spin-Hamiltonian models and were also supported by density functional theory calculations. The presence of frequency-dependent out-of-phase (χ_M'') alternating current susceptibility signals at temperatures below 3 K suggested that **2** might be a single-molecule magnet.

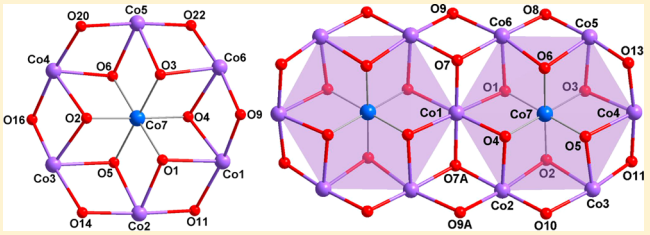

INTRODUCTION

A great number of polynuclear complexes have been synthesized and investigated in the past decade, because of their interesting physical or catalytic properties and especially because of their potential to function as single-molecule magnets (SMMs).[1,2] SMMs not only show properties of classical bulk magnets, but also fascinating quantum mechanical properties, and they have potential applications in information storage and quantum computing.[3] The first SMM, known as Mn_{12}acetate, was published in 1991; it is a mixed-valence oxo−manganese cluster.[4] The synthesis of SMMs is still a tremendous challenge because of the difficulties in assembling predetermined structures with predictable magnetic properties.[5] Maybe a reasonable strategy is to make a smaller cluster whose magnetic property can be controlled, and then extend it to a larger cluster with a foreseeably better magnetic property.

To date, most of the SMMs based on ions with only second-order spin−orbit coupling (e.g., Mn^{III}) are in the strong-exchange limit.[1,6] In this limit, the exchange interactions lead to larger separations between low-lying spin-exchange multiplets than the effects of the magnetic anisotropy.[7] For this type of SMM, the upper limit of the energy barrier for reversal of magnetization is given by $S^2|D|$ or $(S^2 - 1/4)|D|$ for integer and half-integer S values, respectively. Thus, the necessary ingredients are large ground-state spin (S) and significant Ising (easy-axis) types of magnetoanisotropy, as reflected by a negative second-order axial zero-field splitting (ZFS) parameter D. Notably, studies suggested that $|D|$ and S are not completely independent parameters.[8] A promising approach to better SMMs is to move to the weak-exchange limit.[8,9]

In the weak-exchange limit, the magnetic anisotropies of metal ions could be of the same order of magnitude or even larger than the exchange interactions.[6] In this situation, the equation describing the energy barrier by S^2 and D is not applicable, as S is no longer a good quantum number. Evident candidate metal ions for this type of SMM are certain lanthanoid[10] and cobalt(II) ions.[11] Research on such complexes has been an active field recently, and some of the studied complexes exhibited SMM behavior.

Tripodal ligands such as 1,1,1-tris(hydroxymethyl)propane (H_3thmp) have been used extensively in the synthesis of oxo−vanadium clusters, oxo−molybdenum clusters,[12] and paramagnetic 3d transition-metal clusters.[13] We have synthesized a series of $Mn^{III}_4Mn^{II}_8$ clusters via the solvothermal reactions of manganese(II) acetylacetonate ($Mn(acac)_2$), tripodal ligands, and carboxylates.[14] In these compounds, the disposition of the three alkoxide arms of the trianion directs the formation of fused triangular $[Mn_3]$ units, where each arm of the ligand bridges one edge of the triangle. Herein, we present the

Received: December 18, 2013
Published: May 14, 2014

   dx.doi.org/10.1021/ic403093r | Inorg. Chem. 2014, 53, 5458−5466

synthesis, structures, and magnetic properties of two mixed-valence cobalt clusters, $[Co^{III}Co^{II}_6(thmp)_2(acac)_6(ada)_3]$ (**1**) and $[Co^{III}_2Co^{II}_{11}(thmp)_4(Me_3CCO_2)_4(acac)_6(OH)_4(H_2O)_4](Me_3CCO_2)_2\cdot H_2O$ (**2**). Heptanuclear complex **1** was prepared by solvothermal reaction of cobalt(II) acetylacetonate ($Co(acac)_2$), H_3thmp, and adamantane-1-carboxylic acid (Hada). By substituting Hada with Me_3CCO_2H, tridecanuclear complex **2** was obtained under the same reaction conditions. The $[Co^{III}Co^{II}_6]$ core of **1** can be described as a centered hexagon of a central Co^{III} ion surrounded by a Co^{II}_6 hexagon. These kinds of Co_7 disks were widely studied,[11f−i,15] and some of them were confirmed as SMMs.[11f−i] The core structure of **2** can be described as a larger oligomer based on two vertex-sharing $[Co^{III}Co^{II}_6]$ cores. Variable-temperature direct-current (dc) magnetic susceptibility measurements demonstrated overall ferromagnetic coupling between the Co^{II} ions within both clusters. The presence of frequency-dependent out-of-phase (χ_M'') alternating current (ac) susceptibility signals at temperatures below 3 K suggested that **2** might be an SMM.

EXPERIMENTAL SECTION

Materials and General Procedures. All chemicals were commercially available and used as received without further purification. The C, H, and N microanalyses were carried out with an Elementar Vario-EL CHNS elemental analyzer. The Fouriet transform infrared (FT-IR) spectra were recorded from KBr pellets in the range of 4000−400 cm^{-1} on a Bio-Rad FTS-7 spectrometer. Magnetic susceptibility measurements of **1** and **2** were performed with a Quantum Design MPMS-XL7 SQUID magnetometer. Samples were embedded in vaseline to prevent torquing. All the ac susceptibility data were collected at zero dc field and 5 Oe ac amplitude. Data were corrected for the diamagnetic contribution calculated from Pascal constants.

Synthesis. $[Co^{III}Co^{II}_6(thmp)_2(acac)_6(ada)_3]$ (**1**): A mixture of $[Co(acac)_2]$ (0.076 g, 0.30 mmol), H_3thmp (0.026 g, 0.20 mmol), Hada (0.036 g, 0.20 mmol), and MeOH (15 mL) was sealed in a 25 mL Teflon-lined, stainless-steel vessel, heated at 120 °C for 50 h, and then cooled to room temperature. Red block crystals were obtained (yield ca. 42% based on H_3thmp). C, H analysis calcd. (%) for $C_{75}H_{109}Co_7O_{24}$: C 49.84, H 6.08; found (%): C 49.46, H 5.83. Selected IR data (KBr, cm^{-1}): 2906 (m), 2852 (w), 1605 (m), 1557 (m), 1517 (s), 1406 (s), 1309 (w), 1259 (m), 1194 (w), 1116 (w), 1048 (m), 1018 (m), 924 (m), 766 (m), 618 (m), 566 (w).

$[Co^{III}_2Co^{II}_{11}(thmp)_4(Me_3CCOO)_4(acac)_6(OH)_4(H_2O)_4](Me_3CCOO)_2\cdot H_2O$ (**2**): The procedure was the same as that employed for complex **1**, except that Me_3CCOOH (0.020 g, 0.20 mmol) was employed instead of Hada. Red block crystals were obtained (yield ca. 35% based on H_3thmp).C, H analysis calcd. (%) for $C_{84}H_{154}Co_{13}O_{45}$: C 38.06, H 5.86; found (%): C 37.96, H 6.01. Selected IR data (KBr, cm^{-1}): 2959 (m), 2920(m), 2862 (w), 1554 (s), 1520 (s), 1483 (m), 1394 (s), 1260 (w), 1225 (w), 1118 (w), 1055 (m), 1021 (w), 949 (w), 932 (w), 606 (m).

X-ray Structure Determination. Diffraction intensities were collected on a Bruker Apex CCD area-detector diffractometer (Mo Kα, λ = 0.710 73 Å) at 293(2) K. The raw data frames were integrated with the Bruker SAINT package with a narrow frame algorithm.[16] An empirical absorption correction based on symmetry equivalent reflections was applied using the SADABS program.[17] The structures were solved by direct methods, and all non-hydrogen atoms were refined anisotropically by least-squares on F^2 using the SHELXTL program.[18] Anisotropic thermal parameters were assigned to all non-hydrogen atoms. The hydrogen atoms attached to carbon were placed in idealized positions and refined using a riding model to the atom to which they were attached. The H atoms attached to nitrogen and oxygen atoms were experimentally located from the Fourier difference maps and refined with isotropic displacement parameters set to 1.2 × U_{eq} of the attached atoms. Crystal data as well as details of data collection and refinements for complexes are summarized in Table 1. The Oak Ridge thermal ellipsoid plot (ORTEP) plots and packing pictures were produced with Diamond 3.1.[19] Additional crystallographic data can be found in the Supporting Information.

Table 1. Summary of the Crystal Data and Structure Refinement Parameters for 1 and 2

	1	2
formula	$C_{75}H_{109}Co_7O_{24}$	$C_{84}H_{154}Co_{13}O_{45}$
formula weight	1807.13	2650.16
T/K	293(2)	293(2)
color	red block	red block
space group	$P\bar{1}$	$P\bar{1}$
a/Å	12.4752(4)	12.453(2)
b/Å	14.4731(4)	16.319(5)
c/Å	23.9086(8)	16.838(4)
α/deg	97.291(1)	85.465(13)
β/deg	97.813(1)	71.841(7)
γ/deg	93.466(1)	68.454(7)
V/Å^3	4228.9(2)	3022(1)
Z	2	1
D_{calcd}(g·cm^{-3})	1.419	1.456
ref. collected	33 200	53 497
ref. unique	16 171	13 733
R_{int}	0.0439	0.0681
GOF	1.094	1.015
$R_1{}^a$ [$I > 2\sigma(I)$]	0.0647	0.0689
$wR_2{}^b$ [all data]	0.2300	0.2603

$^aR_1 = \sum||F_0| - |F_c||/\sum|F_0|$. $^bwR_2 = \{[\sum w(F_0^2 - F_c^2)^2]/\sum[w(F_0^2)^2]\}^{1/2}$.

DFT Calculations. The density functional theory (DFT) calculations were carried out with the ORCA 3.0 computational package.[20] The hybrid B3LYP functional[21] was used for the calculations of the isotropic exchange constants J following Ruiz's approach[22] by comparing the energies of high-spin (HS) and broken-symmetry (BS) spin states. The polarized triple-ζ quality basis set def2-TZVP(-f) proposed by Ahlrichs and co-workers was used for cobalt and oxygen atoms,[23] while def2-SVP was used for carbon and hydrogen atoms. The calculations utilized the resolution of identity (RI) approximation with the decontracted auxiliary def2-TZV/J or def2-SVP/J Coulomb fitting basis sets and the chain-of-spheres (RIJCOSX) approximation to exact exchange as implemented in ORCA.[24] Increased integration grids (Grid5 and GridX5 in ORCA convention) and strong self-consistent field (SCF) convergence criteria were used in all calculations.

RESULTS AND DISCUSSION

Synthesis. Most of the mixed-valence cobalt clusters were synthesized via room-temperature solution reactions of cobalt(II) salts. These two cobalt clusters were synthesized by the solvothermal reactions, which was not so widely used to prepare discrete molecular clusters other than the metal−organic frameworks (MOFs) and inorganic materials.[25] Superheated solvents exhibit (i) reduced viscosity (and therefore enhanced diffusion of chemical species) and (ii) very different solubilizing properties (e.g., the dielectric constant of water decreases rapidly with increasing temperature)[26] compared to ambient conditions. Note that the vessel was not full of solvent; the Co^{III} ions in the final molecular species might be oxidized by the air in the vessel from Co^{II} acetylacetonate. With unknown brown precipitate obtained with the crystals, the yield of **1** and **2** is not so high.

Crystal Structures. Complex **1** crystallizes in the triclinic space group $P\bar{1}$ with a complete heptanuclear cluster

dx.doi.org/10.1021/ic403093r | Inorg. Chem. 2014, 53, 5458−5466

$[Co_7(thmp)_2(acac)_6(ada)_3]$ (Figure 1a) in the asymmetric unit and a total of two clusters per unit cell (Table 1). Selected

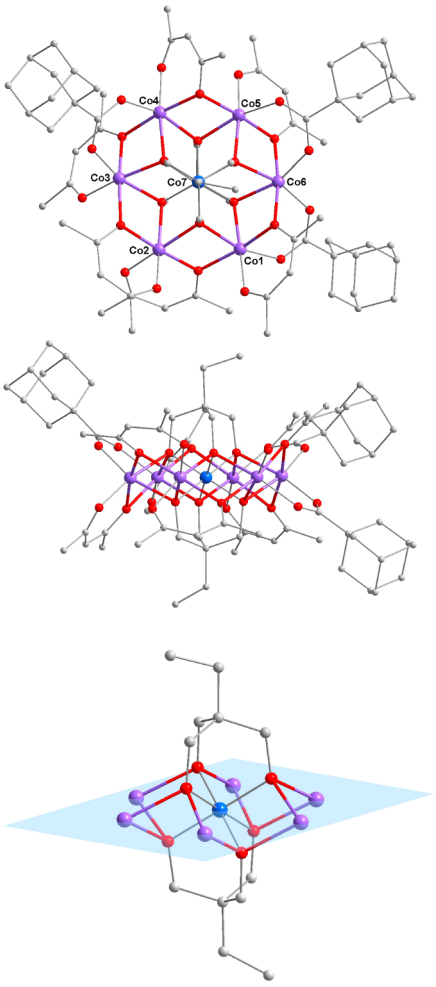

Figure 1. Structure of the $[Co^{III}Co^{II}_6]$ cluster of **1**, viewed perpendicular (a) and parallel (b) to the metal plane. (c) The bridging mode of the two $thmp^{3-}$ ligands above and under the plane. The thicker double-color bonds indicate the magnetic exchange pathways between Co^{II} ions. Color code: Co^{II}, lavender; Co^{III}, light blue; O, red; C, gray.

interatomic distances and angles are listed in Supporting Information, Table S1. All the cobalt ions exhibit identical O_6 environments in distorted octahedral geometries. As the cluster is neutral, charge-balance consideration indicates that one cobalt ion should be in the 3+ valence state and six in the 2+ valence state. As the central Co7 displays evidently shorter bond lengths (1.888−1.915 Å) than the other six Co ions (2.002−2.185 Å), the 3+ valence state is attributed to Co7. Bond valence sum (BVS) calculations[27] were performed for each cobalt center and confirmed this attribution (Supporting Information, Table S2). Thus, the $[Co^{III}Co^{II}_6(\mu_3\text{-}O_{thmp})_6(\mu\text{-}O_{acac})_6]$ core of **1** arranges as a centered hexagon of a central Co^{III} ion surrounded by a Co^{II}_6 hexagon (Figure 2a). Or, the structure can be described as six distorted missing-corner cubanes sharing the neighboring faces of one another (Figure 2b). This disklike core is directed by the two $thmp^{3-}$ ligands that exhibit the $\eta^3,\eta^3,\eta^3,\mu_7$ mode and sit above and below the plane of the seven metal atoms (Figure 1b), with each arm bridging two peripheral Co^{II} ions and the central Co^{III} ion

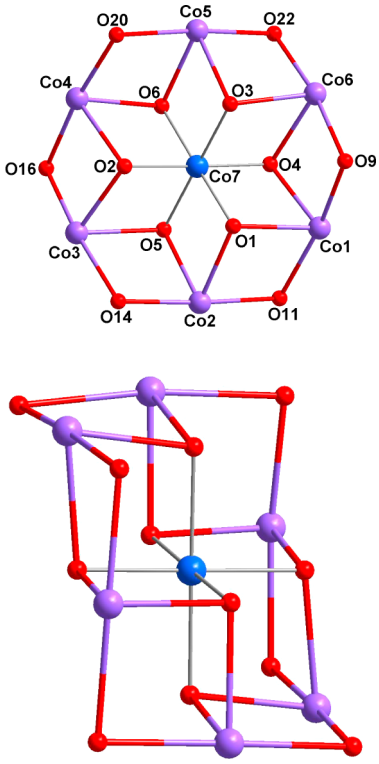

Figure 2. Central core of **1**, viewed perpendicular (a) and parallel (b) to the metal plane.

(Figure 1c). The Co−O−Co angles are in the range of 96.2−100.5°, and the adjacent $Co^{II}\cdots Co^{II}$ distances are 3.17−3.22 Å. Peripheral ligation is provided by three ada^- groups bridging two Co^{II} ions in the common η^1,η^1,μ-bridging mode and six $acac^-$ groups exhibiting the η^1,η^2,μ mode. No significant intermolecular interactions are observed. Notably, two $Co^{III}Co^{II}_6$ clusters, $TBA[Co^{III}Co^{II}_6(thme)_2(O_2CCMe_3)_8Br_2]\cdot MeCN$ and $Na_2[Co^{III}Co^{II}_6(thme)_2(O_2CMe)_{10}(H_2O)_4]\cdot(O_2CMe)\cdot 4.6MeOH\cdot 3H_2O$, based on another tripodal ligand, H_3thme, were reported in 2006.[15a]

Complex **2** crystallizes in the triclinic space group $P\bar{1}$ and consists of a cationic tridecanuclear cluster $[Co^{III}_2Co^{II}_{11}(thmp)_4(Me_3CCOO)_4(acac)_6(OH)_4(H_2O)_4]^{2+}$ (Figure 3a), two Me_3CCOO^- counteranions, and a lattice H_2O. Selected interatomic distances and angles are listed in Supporting Information, Table S3. There are seven independent Co ions, each assuming a distorted octahedral geometry with O_6 environments. Charge-balance considerations and the fact that Co7 displays evidently shorter bond lengths (1.887−1.907 Å) than the other six Co ions (1.979−2.209 Å) indicate the 3+ valence state of Co7, as confirmed by BVS calculations (Supporting Information, Table S2). Thus, the $[Co^{III}_2Co^{II}_{11}(\mu_3\text{-}O)_{14}(\mu_2\text{-}O)_{10}]$ (Figure 4a) core of **2** describes a larger oligomer of the core of **1** based on two centered hexagon $[Co^{III}Co^{II}_6]$ cores sharing a vertical Co1, which lies on the inversion center. Also, the core can be regarded as 14 distorted missing-corner cubanes sharing the neighboring faces of one another (Figure 4b). Again, this disklike core is directed by the four $thmp^{3-}$ ligands that exhibit the $\eta^3,\eta^3,\eta^3,\mu_7$ mode above and below the plane of the 13 metal atoms (Figure 3b). The Co−O−Co angles are in the range of 90.4−102.9°, and the adjacent $Co^{II}\cdots Co^{II}$ distances are 3.04−3.14 Å. BVS calculations were also performed on the inorganic O atoms to assess their

dx.doi.org/10.1021/ic403093r | Inorg. Chem. 2014, 53, 5458−5466

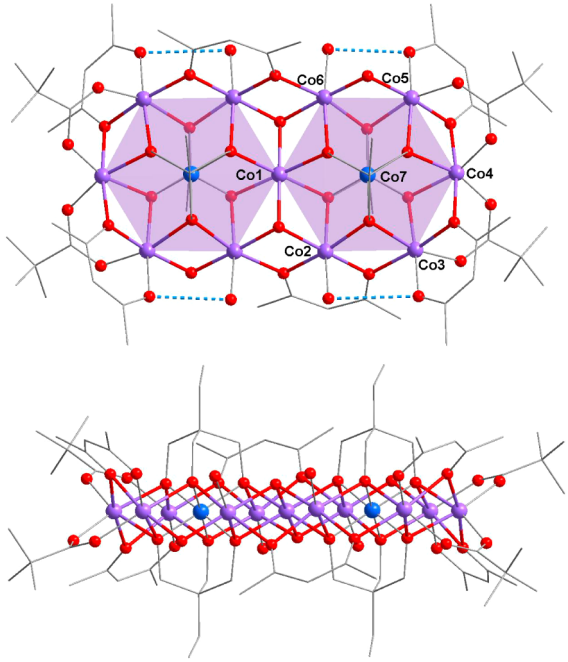

Figure 3. Structure of the $[Co^{III}_2Co^{II}_{11}]$ cluster of **2** viewed perpendicular (a), and parallel (b) to the metal plane. Intramolecular H-bonds are shown as dashed lines.

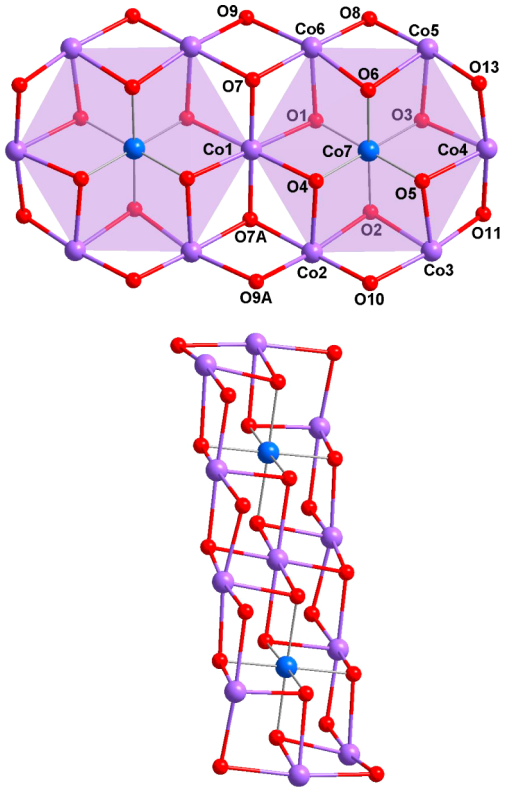

Figure 4. Central core of **2**, viewed perpendicular (a) and parallel (b) to the metal plane. Symmetric codes, A: $-x, -y, 1 - z$.

protonations and suggested two μ_2-OH^- ions (O8 and its symmetry equivalent), two μ_3-OH^- ions (O7 and its symmetry equivalent), and four terminal H_2O ligands (O1W, O2W, and their symmetry equivalent). Peripheral ligation is completed by four pivalate groups and six $acac^-$ groups. Each pivalate group bridges two Co^{II} ions in the common η^1,η^1,μ-bridging mode, while the six $acac^-$ groups exhibit two binding modes: four exhibit the η^1,η^2,μ mode and two adopt a less common η^2,η^2,μ_3 mode. The terminal aqua ligands form H bonds to pivalate ligands, either in the same molecule (Figure 3a), or to pivalate counteranions, which also form H bonds to μ_3-OH^- ions O7 (Figure 5). Again, no significant intercluster interactions can be

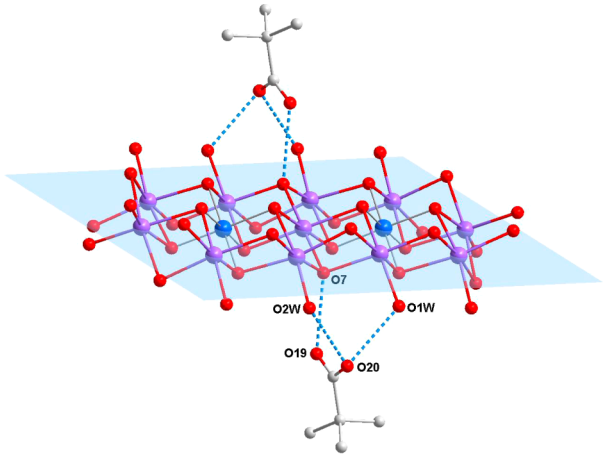

Figure 5. Terminal aqua ligands and μ_3-OH^- ions from H bonds with the pivalate counteranions.

observed. The $[Co^{III}_2Co^{II}_{11}]$ units are well-isolated by pivalate ligands, pivalate counteranions, and H_2O molecules, with the nearest intercluster Co···Co distance of 7.49 Å. This is very important to the confirmation of the SMM nature of **2**, which will be discussed later.

Magnetic Properties. *DFT Study of Complex* ***1****.* Before analyzing the obtained experimental magnetic data of **1**, we performed theoretical calculations of the isotropic exchange constants J_i among paramagnetic Co^{II} atoms based on DFT using B3LYP functional with the help of ORCA. Taking into the account the molecular structure of **1** and presuming that dominant magnetic exchange is mediated between adjacent Co^{II} atoms through oxygen atoms belonging to hydroxo and carboxylate ligands, following spin Hamiltonian was postulated.

$$\hat{H} = -J_{12}(\mathbf{S}_1\cdot\mathbf{S}_2) - J_{23}(\mathbf{S}_2\cdot\mathbf{S}_3) - J_{34}(\mathbf{S}_3\cdot\mathbf{S}_4) - J_{45}(\mathbf{S}_4\cdot\mathbf{S}_5) - J_{56}(\mathbf{S}_5\cdot\mathbf{S}_6) - J_{16}(\mathbf{S}_1\cdot\mathbf{S}_6) \quad (1)$$

To be able to analyze all six potential magnetic exchange interactions J_{ij}, the several BS spin states were calculated as outlined in Supporting Information, Table S4. In HS and BS spin states, most of the spin density was localized on Co^{II} atoms and partially also on oxygen atoms of corresponding CoO6 chromophores. By following Ruiz's approach for calculation of *J*-parameters, we derived these expressions for individual *J*-values:

dx.doi.org/10.1021/ic403093r | Inorg. Chem. 2014, 53, 5458−5466

$$J_{12} = (\Delta_1 + \Delta_2 - \Delta_{12})/12$$
$$J_{23} = (-\Delta_1 + \Delta_2 + \Delta_{12})/12$$
$$J_{34} = (\Delta_1 - \Delta_2 + 2\Delta_3 - \Delta_{12})/12$$
$$J_{45} = (-\Delta_1 + \Delta_2 - 2\Delta_3 + 2\Delta_4 + \Delta_{12})/12$$
$$J_{56} = (\Delta_1 - \Delta_2 + 2\Delta_3 - 2\Delta_4 + 2\Delta_5 - \Delta_{12})/12$$
$$J_{16} = (\Delta_1 - \Delta_2 + \Delta_{12})/12 \quad (2)$$

where Δ_i is the energy difference between each BS spin state and HS state. The analysis resulted in these isotropic exchange constants: $J_{12} = -0.40$ cm^{-1}, $J_{23} = +1.54$ cm^{-1}, $J_{34} = +3.88$ cm^{-1}, $J_{45} = +6.36$ cm^{-1}, $J_{56} = +1.10$ cm^{-1}, and $J_{16} = +11.38$ cm^{-1}. Thus, these results show that the ferromagnetic exchange is prevailing in compound **1**. Furthermore, the magnetic exchange pathways can be divided into two groups; in the first one the magnetic exchange between Co(II) is mediated by two bridging oxygen atoms belonging to thmp and acac ligands, [Co$_i$(μ_3-O$_{thmp}$)(μ-O$_{acac}$)Co$_j$] (i–j = 1–2, 2–3, and 4–5), while in the second group, the carboxylic group of the ada ligand is also involved, [Co$_i$(μ_3-O$_{thmp}$)(μ-O$_{acac}$)(μ-O,O$_{ada}$)Co$_j$] (i–j = 1–6, 3–4, and 5–6). In both groups, the correlation between averaged Co–O–Co angles and calculated J-values is evident (Figure 6).

Magnetic Properties of Complex 1. Variable-temperature and dc magnetic susceptibility measurements were performed on a microcrystalline powder sample of **1** in a 500 G (0.05 T) field and in the 1.8–300 K range, and also the isothermal magnetization at 1.8 K was measured up to maximum magnetic field of 7 T. The obtained data are shown in Figure 7. The μ_{eff} value of 12.69 μ_B is much larger than the spin-only (S = 3/2, g = 2) value of six noninteracting HS Co^{II} ions (9.49 μ_B), due to the significant spin–orbit coupling of the octahedral Co^{II} ions. The value decreases gradually to a minimum at T = 40 K and then increases sharply to reach a value of 14.57 μ_B at T = 4 K. For HS Co^{II} ions with distorted octahedral symmetry, the only level that populated at sufficiently low temperature is the lowest-lying Kramer's doublet corresponding to an effective spin S' = 1/2, with effective anisotropic g' values.[28] So, the decrease of μ_{eff} before 40 K can be attributed to such spin–orbit coupling and low-symmetry ligand field effects, while the sharp increase below 40 K indicates ferromagnetic exchange coupling between metallic centers. The maximum μ_{eff}/μ_B value at 4 K corresponds to six ferromagnetic coupled Co^{II} ions each with an effective S' = 1/2 state and a g' value of 4.2. The sudden decrease below 4 K could be attributed mainly to the field saturation effect. The fast-increased variation on isothermal field-dependent magnetization versus magnetic field further confirms the intramolecular ferromagnetic coupling. The saturation value $M_{mol}/N_A\mu_B$ at B = 7.0 T equals 13.9, which is much less than the theoretical value of 18.0 for six HS Co^{II} ions (S = 3/2, g = 2), thus confirming large ZFS of cobalt(II) ions.

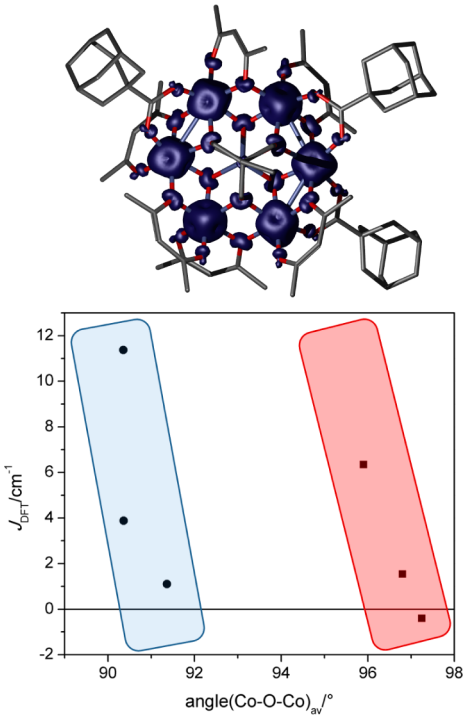

Figure 6. (top) The calculated spin density distribution using B3LYP of compound **1** for the HS state. Positive spin density is represented by blue surface. The isodensity surfaces are plotted with the cutoff values of 0.01 e a_0^{-3}. (bottom) The DFT-based J-values vs averaged Co–O–Co angles, where ■ represents J_{ij}-values for [Co$_i$(μ_3-O$_{thmp}$)(μ-O$_{acac}$)Co$_j$] (i–j = 1–2, 2–3, and 4–5) pairs and ● represents J_{ij}-values for [Co$_i$(μ_3-O$_{thmp}$)(μ-O$_{acac}$)(μ-O,O$_{ada}$)Co$_j$] (i–j = 1–6, 3–4, and 5–6) pairs. The red and blue oblong shapes serve as a guide for eyes.

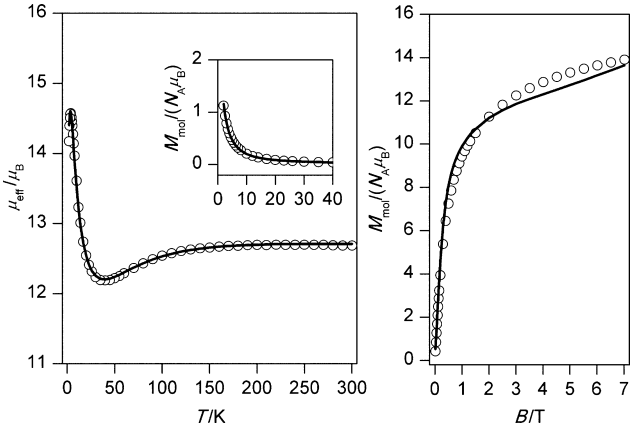

Figure 7. Magnetic data for **1**. (left) The temperature dependence of the effective magnetic moment and molar magnetization measured at B = 0.05 T. (right) The isothermal magnetizations measured at T = 1.8. Empty circles—experimental data, full lines—calculated data using eq 3, with J_a = +0.95 cm^{-1}, J_b = 5.11 cm^{-1}, D = 79.3 cm^{-1}, and g = 2.65.

To quantitatively determine the isotropic exchange and the ZFS parameters in **1**, and taking into account results from DFT analysis, the following spin Hamiltonian was used.

$$\hat{H} = -J_a(\mathbf{S}_1\cdot\mathbf{S}_2 + \mathbf{S}_2\cdot\mathbf{S}_3 + \mathbf{S}_5\cdot\mathbf{S}_6) - J_b(\mathbf{S}_3\cdot\mathbf{S}_4 + \mathbf{S}_4\cdot\mathbf{S}_5 + \mathbf{S}_6\cdot\mathbf{S}_1) + \sum_{i=1}^{6}\mathbf{S}_i\cdot\mathbf{D}_i\cdot\mathbf{S}_i + \mu_B\sum_{i=1}^{6}\mathbf{B}\cdot\mathbf{g}_i\cdot\mathbf{S}_i \quad (3)$$

where J_a represents weaker averaged isotropic exchange between Co1–Co2, Co2–Co3, and Co5–Co6 atoms, and J_b represents stronger averaged isotropic exchange among the rest of the cobalt couples. The third term in eq 1 represents ZFS, where we assumed that the **D**-tensor is equal for all cobalt(II) atoms and is parametrized with single-ion axial ZFS parameter

dx.doi.org/10.1021/ic403093r | Inorg. Chem. 2014, 53, 5458–5466

Table 2. Summary of Structural and Magnetic Parameters for 1

Co_i–Co_j	d(Co_i–Co_j) (Å)	∠(Co_i–O–Co_j) (deg)	∠(Co_i–O–Co_j)$_{av.}$ (deg)	J_i^{DFT} (cm^{-1})	J_i^{MAG} (cm^{-1})[a]
Co1–Co2	3.174	95.60	97.25	−0.40	+0.95
		98.90			
Co2–Co3	3.169	94.70	96.80	+1.54	+0.95
		98.90			
Co3–Co4	3.022	90.03	90.36	+3.88	+5.11
		90.69			
Co4–Co5	3.145	95.06	95.91	+6.36	+5.11
		96.75			
Co5–Co6	3.034	91.05	91.36	+1.10	+0.95
		91.67			
Co6–Co1	3.038	89.13	90.35	+11.38	+5.11
		91.58			

[a]The experimental magnetic data were fitted with averaged J-parameter, $J_a = J_{12} = J_{23} = J_{56}$ and $J_b = J_{34} = J_{45} = J_{16}$.

D. Also, the isotropic g-value was assumed in the Zeeman term. The spin Hamiltonian then acted on local spin basis set $|S_1, M_{S1}\rangle \cdots |S_6, M_{S6}\rangle$, which ended in matrices with dimension of 4096 × 4096. The diagonalization of such matrices for a given set of parameters (J_a, J_b, D, and g) and for given magnetic fields enabled us to obtain eigenvalues and, hence, partition function Z, which was used to calculate molar magnetization as $M_{mol} = N_A kT\ d(\ln(Z))/d(B)$. The magnetization for powder sample was then calculated as an arithmetic average $M_{mol} = (2M_x + M_z)/3$. Next, the four parameters were varied to obtain the best agreement between experimental and calculated magnetic data (both temperature and field dependent), which resulted in J_a = +0.95 cm^{-1}, J_b = 5.11 cm^{-1}, D = 79.3 cm^{-1}, and g = 2.65 (Figure 7). The J-values are in qualitative agreement with averaged DFT calculated parameters (J_a^{DFT} = +0.75 cm^{-1}, J_b^{DFT} = 7.21 cm^{-1}), which emphasize the importance of theoretical methods in magnetic analysis of complex systems. Also, the large D-value and g-factor agree well with distorted octahedral chromophore of cobalt(II) ions and significant spin–orbit coupling. The fitted parameters clearly confirmed that weak-exchange limit, $|D| \gg |J_i|$, is present in compound **1** (Table 2), so the spin S is no longer a good quantum number, and the energy pattern is dominated by ZFS parameter D, as demonstrated in Supporting Information, Figure S1.

Furthermore, to investigate whether complex **1** might be SMM, ac susceptibility measurements were performed in a 5 G ac field oscillating at 1–1500 Hz and with a zero applied dc field (Supporting Information, Figure S2). Unfortunately, no out-of-phase (χ_M'') ac signal is observed.

Magnetic Properties of Complex **2**. Variable-temperature dc magnetic susceptibility data for complex **2** were collected as for **1** and are shown in Figure 8. Again, the room-temperature μ_{eff} value (17.20 μ_B) is much larger than the spin-only (S = 3/2, g = 2) value of 11 HS Co^{II} ions (12.85 μ_{eff}/μ_B). The value slowly increases until T = 140 K, then decreases gradually to a minimum at T = 55 K, and then increases sharply to 23.38 μ_{eff}/μ_B at T = 3.5 K. The gentle increase and decrease before 55 K could be attributed to the competition between the spin–orbit coupling of the Co^{II} ions and the overall ferromagnetic intracluster exchange. The latter is clearly revealed by the sharp increase below 55 K. The maximum μ_{eff} value at 3.5 K corresponds to 11 ferromagnetic coupled Co^{II} ions each with an effective S' = 1/2 state and a g' value of 3.9. The sudden decrease below 3.5 K could be attributed to the field saturation effect. As with complex **1**, the fast-increased variation on the isothermal field-dependent magnetization versus B further

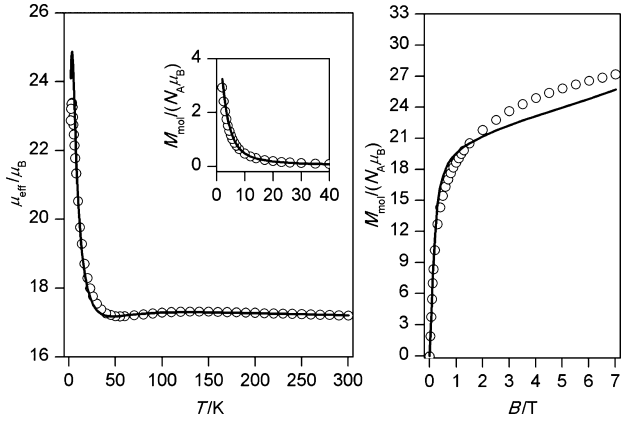

Figure 8. Magnetic data for **2**. (left) The temperature dependence of the effective magnetic moment and molar magnetization measured at B = 0.05 T. (right) The isothermal magnetizations measured at T = 1.8. Empty circles–experimental data, full lines–calculated data using eq 4, with J = 3.34 cm^{-1}, D = 63.8 cm^{-1}, and g = 2.64.

confirms the intermolecular ferromagnetic coupling. At T = 1.8 K and B = 7.0 T, the $M_{mol}/N_A\mu_B$ value reaches a maximum that equals 27.2, which is lower than the theoretical value of 33.0 for 11 HS Co^{II} ions (S = 3/2, g = 2), thus again confirming large ZFS of cobalt(II) ions.

In the case of compound **2**, magnetic analysis requires knowledge about of $(2S_i + 1)^{11} = 4^{11} = 4\ 194\ 304$ magnetic states, which is beyond the capabilities of exact diagonalization techniques. Therefore, to provide some estimates of magnetic parameters within this compound, we approximate its magnetic properties with a model usually adopted for one-dimensional (1D) chains—the model of finite-size closed ring with spin Hamiltonian

$$\hat{H} = -J\sum_{i=1}^{N-1}(\mathbf{S}_i\cdot\mathbf{S}_{i+1}) - J(\mathbf{S}_N\cdot\mathbf{S}_1) + \sum_{i=1}^{N}\mathbf{S}_i\cdot\mathbf{D}_i\cdot\mathbf{S}_i + \mu_B\sum_{i=1}^{N}\mathbf{B}\cdot\mathbf{g}_i\cdot\mathbf{S}_i \quad (4)$$

It usually holds that the larger the value of N is, the better the approximation to infinite 1D chain. However, including ZFS term means that knowledge about all magnetic states is necessary. This restricted us to N = 7, which resulted in 4^7 = 16 384 magnetic levels. To efficiently calculate magnetic properties for different temperatures and magnetic fields and for varying

dx.doi.org/10.1021/ic403093r | Inorg. Chem. 2014, 53, 5458–5466

parameters (J, D, g), many diagonalizations are required. Therefore, the spin permutational symmetry of the spin Hamiltonian was used, and a new set of symmetry-adapted spin basis set was created using D_7 point group.[29] Such procedure split the total interaction matrix into submatrices A_1 (N = 1300), A_2 (N = 1044), E_1 (N = 4680), E_2 (N = 4680), and E_3 (N = 4680), labeled using the irreducible representations.[30] Then, the fitting procedure based on both temperature and field-dependent magnetic data resulted in J = 3.34 cm^{-1}, D = 63.8 cm^{-1}, and g = 2.64 (Figure 8). Even though the overall fit shows some deviations from experimental data, the obtained values confirmed dominant ferromagnetic coupling within this compound and significant ZFS of Co(II) ions similar to compound **1**.

Furthermore, ac susceptibility measurements were performed for complex **2** in a 5 G ac field oscillating at 1−1500 Hz and with a zero applied dc field (Figure 9). Clearly nonzero and

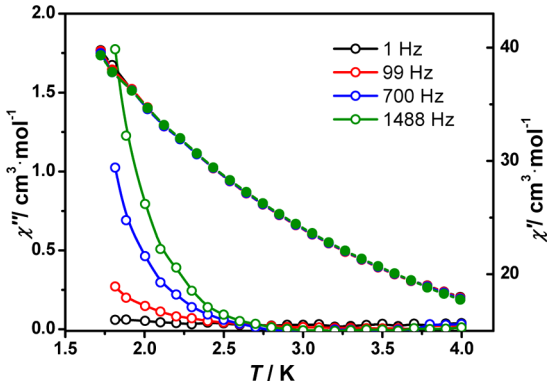

Figure 9. Temperature dependence of the in-phase (χ'_M, ●) and out-of-phase (χ''_M, ○) ac susceptibility signals under zero dc field at the indicated frequencies for **2**.

frequency-dependent out-of-phase (χ_M'') ac signal was observed below 3 K, indicating a slow relaxation of the magnetization. However, no peak in χ_M'' is seen even down to 1.8 K, the limit of our magnetometer. Under a dc field of 1000 Oe, the in-phase ac susceptibility signals clearly show frequency-dependence, while the peak of χ_M'' is still absent (Supporting Information, Figure S3).

DISCUSSION

The disklike cobalt clusters have been widely studied and synthesized with different ligands and oxidation levels such as $[Co^{II}_7]$,[11f−h,15a] $[Co^{III}Co^{II}_6]$,[15b] $[Co^{III}_3Co^{II}_4]$,[11i,15c,d] $[Co^{III}_4Co^{II}_3]$,[15e] and $[Co^{II}_9Co^{III}_3]$[15f] (Figure 10). On the other hand, these disklike cores can be described as many

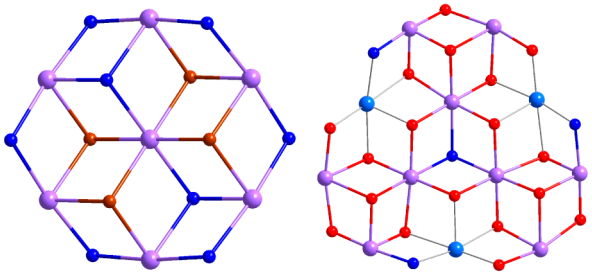

Figure 10. Core structures of $[Co^{II}_7]$[11f] (left) and $[Co^{II}_9Co^{III}_3]$[15f] (right). Color code: Co^{II}, lavender; Co^{III}, light blue; O, red; N, blue.

distorted missing-corner cubanes sharing the neighboring faces of one another. To the best of our knowledge, the $[Co^{III}_2Co^{II}_{11}]$ cluster reported here is one of the biggest disklike cobalt clusters.[31] Notably, all the overall intracluster exchanges between the Co^{II} ions within the reported cobalt disks are ferromagnetic, except $[Co^{II}_9Co^{III}_3]$.[15f] This might be directed by the inner μ_3-N/O atoms, which sit above and below the metal disks. The coplane arrangement of the Co ions restricts these Co−(μ_3-)N/O−Co angles to 89.4−100°, while for $[Co^{II}_9Co^{III}_3]$, the cobalt ions are not strictly coplane arranged, leading to a 103.5° angle (Supporting Information, Table S3). It was known that (i) the ferromagnetic exchange pathways are dominant in the range of 90−100° and (ii) large superexchange angles lead to antiferromagnetic interactions, while smaller ones induce ferromagnetic coupling.[32] For complex **1** and **2**, the inner μ_3-O are supplied by thmp^{3-}, and the Co−(μ_3-)O−Co angles are in the range of 89.9−96.5°.

CONCLUSION

The use of tripodal ligand H_3thmp and different carboxylates represents a strategy for assembling high-nuclearity ferromagnetic cobalt clusters. This work demonstrates the synthesis and magnetic studies of two disklike cobalt clusters. The tridecanuclear complex **2** was obtained via substituting the carboxylate ligands of heptanuclear complex **1**. The core structure of **2** can be described as a larger oligomer based on two vertex-sharing $[Co^{III}Co^{II}_6]$ cores. More significantly, the tridecanuclear cluster inherited the ferromagnetic manner of the heptanuclear cluster. Thus, a larger ferromagnetic cluster was obtained. The advanced magnetic analysis, supported by DFT calculations in case of **1**, provided us with valuable information about isotropic exchange and ZFS parameters presented in such complicated structures. Furthermore, complex **2** shows slow magnetic relaxation at static zero and 1000 Oe fields below 4 K, toward SMM behavior. The reason why we see SMM-like behavior in **2** and not in **1** may be complex; however, we can speculate that main reasons lie in small but significant changes in chromophore geometries of paramagnetic Co(II) ions and slight modifications of exchange pathways resulting in change of spin-reversal energy barrier.

ASSOCIATED CONTENT

Supporting Information

Selected bonds and angles in **1** and **2** and BVS for selected O atoms in **1** and **2**. This material is available free of charge via the Internet at http://pubs.acs.org. CCDC 975537 (**1**) and 975538 (**2**) contain the supplementary crystallographic data for this Paper. These data can be obtained free of charge from the Cambridge Crystallographic Data Center via www.ccdc.cam.ac.uk/data_request/cif.

AUTHOR INFORMATION

Corresponding Authors

*E-mail: tongml@mail.sysu.edu.cn. (M.L.T.)
*E-mail: radovan.herchel@upol.cz. (R.H.)

Notes

The authors declare no competing financial interest.

ACKNOWLEDGMENTS

This work was supported by the "973 Project" (2012CB821704 and 2014CB845602), the National Natural Science Foundation of China (Grant Nos. 91122032, 21201182 and 21121061),

and Program for Changjiang Scholars and Innovative Research Team in University of China (IRT1298) China (IRT1298) and by the Operational Program Research and Development for Innovations (CZ.1.05/2.1.00/03.0058) of the Ministry of Education, Youth and Sports of the Czech Republic.

REFERENCES

(1) For reviews, see (a) Christou, G.; Gatteschi, D.; Hendrickson, D. N.; Sessoli, R. *MRS Bull.* **2000**, *25*, 66. (b) Gatteschi, D.; Sessoli, R. *Angew. Chem., Int. Ed.* **2003**, *43*, 268. (c) Aromí, G.; Brechin, E. K. *Struct. Bonding (Berlin, Ger.)* **2006**, *122*, 1.

(2) (a) Sessoli, R.; Gatteschi, D.; Caneschi, A.; Novak, M. A. *Nature* **1993**, *365*, 141. (b) Shores, M. P.; Sokol, J. J.; Long, J. R. *J. Am. Chem. Soc.* **2002**, *124*, 2279. (c) Schelter, E. J.; Prosvirin, A. V.; Dunbar, K. R. *J. Am. Chem. Soc.* **2004**, *126*, 15004. (d) Oshio, H.; Nihei, M.; Koizumi, S.; Shiga, T.; Nojiri, H.; Nakano, M.; Shirakawa, N.; Akatsu, M. *J. Am. Chem. Soc.* **2005**, *127*, 4568. (e) Wang, W.-G.; Zhou, A.-J.; Zhang, W.-X.; Tong, M.-L.; Chen, X.-M.; Nakano, M.; Beedle, C. C.; Hendrickson, D. N. *J. Am. Chem. Soc.* **2007**, *129*, 1014. (f) Liu, J.-L.; Guo, F.-S.; Meng, Z.-S.; Zheng, Y.-Z.; Leng, J.-D.; Tong, M.-L.; Ungur, L.; Chibotaru, L. F.; Heroux, K. J.; Hendrickson, D. N. *Chem. Sci.* **2011**, *2*, 1268.

(3) (a) Friedman, J. R.; Sarachik, M. P.; Tejada, J.; Ziolo, R. *Phys. Rev. Lett.* **1996**, *76*, 3830. (b) Thomas, L.; Lionti, L.; Ballou, R.; Gatteschi, D.; Sessoli, R.; Barbara, B. *Nature* **1996**, *383*, 145. (c) Timco, G. A.; Carretta, S.; Troiani, F.; Tuna, F.; Pritchard, R. J.; Muryn, C. A.; McInnes, E. J. L.; Ghirri, A.; Candini, A.; Santini, P.; Amoretti, G.; Affronte, M.; Winpenny, R. E. P. *Nat. Nanotechnol.* **2009**, *4*, 173. (d) Hill, S.; Datta, S.; Liu, J.; Inglis, R.; Milios, C. J.; Feng, P. L.; Henderson, J. J.; del Barco, E.; Brechin, E. K.; Hendrickson, D. N. *Dalton Trans.* **2010**, *39*, 4693.

(4) Caneschi, A.; Gatteschi, D.; Sessoli, R. *J. Am. Chem. Soc.* **1991**, *113*, 5873.

(5) From the Molecular to the Nanoscale. In *Synthesis, Structure, and Properties;* Fujita, M., Powell, A., Creutz, C., Eds.; Elsevier: Oxford, U.K., 2004; Vol. 7.

(6) Bencini, A.; Gatteschi, D. *EPR of Exchange Coupled Systems;* Springer: Berlin, Germany, 1990.

(7) (a) Gatteschi, D.; Sessoli, R.; Villain, J. *Molecular Nanomagnets;* Oxford University Press: Oxford, U.K., 2006. (b) Cornia, A.; Gatteschi, D.; Sessoli, R. *Coord. Chem. Rev.* **2001**, *219*−*221*, 573.

(8) Waldmann, O. *Inorg. Chem.* **2007**, *46*, 10035.

(9) Murrie, M. *Chem. Soc. Rev.* **2010**, *39*, 1986.

(10) For examples, see (a) Westin, L. G.; Kritikos, M.; Caneschi, A. *Chem. Commun.* **2003**, 1012. (b) Ishikawa, N.; Sugita, M.; Wernsdorfer, W. *J. Am. Chem. Soc.* **2005**, *127*, 3650. (c) Tang, J.-K.; Hewitt, I.; Madhu, N. T.; Chastanet, G.; Wernsdorfer, W.; Anson, C. E.; Benelli, C.; Sessoli, R.; Powell, A. K. *Angew. Chem., Int. Ed.* **2006**, *45*, 1729. (d) Lin, P.-H.; Burchell, T. J.; Clérac, R.; Murugesu, M. *Angew. Chem., Int. Ed.* **2008**, *47*, 8848. (e) Zheng, Y.-Z.; Lan, Y.-H.; Anson, C. E.; Powell, A. K. *Inorg. Chem.* **2008**, *47*, 10813. (f) Guo, Y.-N.; Xu, G.-F.; Gamez, P.; Zhao, L.; Lin, S.-Y.; Deng, R.-P.; Tang, J.-K.; Zhang, H.-J. *J. Am. Chem. Soc.* **2010**, *132*, 8538. (g) Guo, F.-S.; Liu, J.-L.; Leng, J.-D.; Tong, M.-L.; Gao, S.; Ungur, L.; Chibotaru, L. F. *Chem.—Eur. J.* **2011**, *17*, 2458. (h) Liu, J.-L.; Chen, Y.-C.; Zhen, Y.-Z.; Lin, W.-Q.; Ungur, L.; Wernsdorfer, W.; Chibotaru, L. F.; Tong, M.-L. *Chem. Sci.* **2013**, *4*, 3310.

(11) Co3 (a) Zhu, Y.-Y.; Cui, C.; Zhang, Y.-Q.; Jia, J.-H.; Guo, X.; Gao, C.; Qian, K.; Jiang, S.-D.; Wang, B.-W.; Wang, Z.-M.; Gao, S. *Chem. Sci.* **2013**, *4*, 1802. Co4 (b) Yang, E.-C.; Wernsdorfer, W.; Nakano, M.; Zakharov, L. N.; Sommer, R. D.; Rheingold, A. L.; Ledezma-Gairaud, M.; Christou, G. *J. Appl. Phys.* **2002**, *91*, 7382. (c) Galloway, K. W.; Whyte, A. M.; Wernsdorfer, W.; Sanchez-Benitez, J.; Kamenev, K. V.; Parkin, A.; Peacock, R. D.; Murrie, M. *Inorg. Chem.* **2008**, *47*, 7438. (d) Wu, D.; Guo, D.; Song, Y.; Huang, W.; Duan, C.; Meng, Q.; Sato, O. *Inorg. Chem.* **2009**, *48*, 854. Co5 (e) Klöwer, F.; Lan, Y.-H.; Nehrkorn, J.; Waldmann, O.; Anson, C. E.; Powell, A. K. *Chem.—Eur. J.* **2009**, *15*, 7413. Co6 (f) Murrie, M.; Teat, S. J.; Stoeckli-Evans, H.; Güdel, H. U. *Angew. Chem., Int. Ed.* **2003**, *42*, 4653. Co7 (g) Zhang, Y.-Z.; Wernsdorfer, W.; Pan, F.; Wang, Z.-M.; Gao, S. *Chem. Commun.* **2006**, 3302. (h) Wang, X.-T.; Wang, B.-W.; Wang, Z.-M.; Zhang, W.; Gao, S. *Inorg. Chim. Acta* **2008**, *361*, 3895. (i) Zhou, Y.-L.; Zeng, M.-H.; Wei, L.-Q.; Li, B.-W.; Kurmoo, M. *Chem. Mater.* **2010**, *22*, 4295. (j) Ferguson, A.; Parkin, A.; Sanchez-Benitez, J.; Kamenev, K.; Wernsdorfer, W.; Murrie, M. *Chem. Commun.* **2007**, 3473. Co8 (k) Langley, S. J.; Helliwell, M.; Sessoli, R.; Rosa, P.; Wernsdorfer, W.; Winpenny, R. E. P. *Chem. Commun.* **2005**, 5029. (l) Moubaraki, B.; Murray, K. S.; Hudson, T. A.; Robson, R. *Eur. J. Inorg. Chem.* **2008**, 4525. Co12 (m) Zeng, M.-H.; Yao, M.-X.; Liang, H.; Zhang, W.-X.; Chen, X.-M. *Angew. Chem., Int. Ed.* **2007**, *46*, 1832. (n) Zhou, Y.-L.; Zeng, M.-H.; Liu, X.-C.; Liang, H.; Kurmoo, M. *Chem.—Eur. J.* **2011**, *17*, 14084. Co16 (o) Hu, Y.-Q.; Zeng, M.-H.; Zhang, K.; Hu, S.; Zhou, F.-F.; Kurmoo, M. *J. Am. Chem. Soc.* **2013**, *135*, 7901.

(12) (a) Khan, M. I.; Zubieta, J. *Prog. Inorg. Chem.* **1995**, *43*, 1. (b) Cavaluzzo, M.; Chen, Q.; Zubieta, J. *J. Chem. Soc., Chem. Commun.* **1993**, 131. (c) Finn, R. C.; Zubieta, J. *J. Cluster Sci.* **2000**, *11*, 461. (d) Saalfrank, R. W.; Bernt, I.; Uller, E.; Hampel, F. *Angew. Chem., Int. Ed. Engl.* **1997**, *36*, 2482.

(13) (a) Jones, L. F.; Batsanov, A.; Brechin, E. K.; Collison, D.; Helliwell, M.; Mallah, T.; McInnes, E. J. L.; Piligkos, S. *Angew. Chem., Int. Ed.* **2002**, *41*, 4318. (b) Moragues-Canovas, M.; Helliwell, M.; Ricard, L.; Rivière, É.; Wernsdorfer, W.; Brechin, E. K.; Mallah, T. *Eur. J. Inorg. Chem.* **2004**, 2219. (c) Rajaraman, G.; Murugesu, M.; Sanudo, E. C.; Soler, M.; Wernsdorfer, W.; Helliwell, M.; Muryn, C.; Raftery, J.; Teat, S. J.; Christou, G.; Brechin, E. K. *J. Am. Chem. Soc.* **2004**, *126*, 15445. (d) Brechin, E. K. *Chem. Commun.* **2005**, 5141. (e) Li, Y.-G.; Wernsdorfer, W.; Clérac, R.; Hewitt, I. J.; Anson, C. E.; Powell, A. K. *Inorg. Chem.* **2006**, *45*, 2376. (f) Liu, C.-M.; Zhang, D.-Q.; Zhu, D.-B. *Inorg. Chem.* **2009**, *48*, 792.

(14) (a) Leng, J.-D.; Dian, L.-Y.; Liu, J.-L.; Tong, M.-L. *Eur. J. Inorg. Chem.* **2011**, 2317. (b) Leng, J.-D.; Dian, L.-Y.; Liu, J.-L.; Tong, M.-L. *Polyhedron* **2011**, *30*, 3088.

(15) (a) Wei, L.-Q.; Li, B.-W.; Hu, S.; Zeng, M.-H. *CrystEngComm* **2011**, *13*, 510. (b) Moragues-Canovas, M.; Talbot-Eeckelaers, C. E.; Catala, L.; Lloret, F.; Wernsdorfer, W.; Brechin, E. K.; Mallah, T. *Inorg. Chem.* **2006**, *45*, 7038. (c) Alley, K. G.; Bircher, R.; Waldmann, O.; Ochsenbein, S. T.; Gudel, H. U.; Moubaraki, B.; Murray, K. S.; Fernandez-Alonso, F.; Abrahams, B. F.; Boskovic, C. *Inorg. Chem.* **2006**, *45*, 8950. (d) Tudor, V.; Marin, G.; Lloret, F.; Kravtsov, V. Ch.; Simonov, Y. A.; Julve, M.; Andruh, M. *Inorg. Chim. Acta* **2008**, *361*, 3446. (e) Chibotaru, L. F.; Ungur, L.; Aronica, C.; Elmoll, H.; Pilet, G.; Luneau, D. *J. Am. Chem. Soc.* **2008**, *130*, 12445. (f) Zheng, L.-L.; Leng, J.-D.; Herchel, R.; Lan, Y.-H.; Powell, A. K.; Tong, M.-L. *Eur. J. Inorg. Chem.* **2010**, 2229.

(16) Blessing, R. H. *Acta Crystallogr., Sect. A* **1995**, *51*, 33.

(17) Sheldrick, G. M. *SADABS 2.05;* University Göttingen: Gottingen, Germany, 1997.

(18) *SHELXTL 6.10;* Bruker Analytical Instrumentation: Madison, WI, 2000.

(19) Pennington, W. T. *J. Appl. Crystallogr.* **1999**, *32*, 1028.

(20) (a) Neese, F. *ORCA—an ab initio, Density Functional and Semiempirical Program Package, 3.0.1;* University of Bonn: Bonn, Germany, 2013. http://www.thch.uni-bonn.de/tc/orca/. (b) Neese, F. *WIREs Comput. Mol. Sci.* **2012**, *2*, 73.

(21) (a) Lee, C.; Yang, W.; Parr, R. G. *Phys. Rev. B* **1988**, *37*, 785. (b) Becke, A. D. *J. Chem. Phys.* **1993**, *98*, 1372. (c) Becke, A. D. *J. Chem. Phys.* **1993**, *98*, 5648. (d) Stephens, P. J.; Devlin, F. J.; Chabalowski, C. F.; Frisch, M. J. *J. Phys. Chem.* **1994**, *98*, 11623.

(22) (a) Ruiz, E.; Cano, J.; Alvarez, S.; Alemany, P. *J. Comput. Chem.* **1999**, *20*, 1391. (b) Ruiz, E.; Rodríguez-Fortea, A.; Cano, J.; Alvarez, S.; Alemany, P. *J. Comput. Chem.* **2003**, *24*, 982.

(23) (a) Schafer, A.; Horn, H.; Ahlrichs, R. *J. Chem. Phys.* **1992**, *97*, 2571. (b) Schafer, A.; Huber, C.; Ahlrichs, R. *J. Chem. Phys.* **1994**, *100*, 5829. (c) Weigend, F.; Ahlrichs, R. *Phys. Chem. Chem. Phys.* **2005**, *7*, 3297.

(24) (a) Neese, F.; Wennmohs, F.; Hansen, A.; Becker, U. *Chem. Phys.* **2009**, *356*, 98. (b) Izsak, R.; Neese, F. *J. Chem. Phys.* **2011**, *135*, 144105.
(25) Laye, R.; McInnes, E. J. L. *Eur. J. Inorg. Chem.* **2004**, 2811.
(26) Rabenau, A. *Angew. Chem., Int. Ed. Engl.* **1985**, *24*, 1026.
(27) (a) Brown, I. D.; Altermatt, D. *Acta Crystallogr.* **1985**, *B41*, 244. (b) Brese, N. E.; O'Keeffe, M. *Acta Crystallogr.* **1991**, *B47*, 192. (c) Liu, W.; Thorp, H. H. *Inorg. Chem.* **1993**, *32*, 4102.
(28) (a) Banci, L.; Bencini, A.; Benelli, C.; Gatteschi, D.; Zanchini, C. *Struct. Bonding (Berlin, Ger.)* **1982**, *52*, 37. (b) Kahn, O. *Molecular Magnetism;* VCH Publishers: New York, 1993.
(29) (a) Waldmann, O. *Phys. Rev. B: Condens. Matter Mater. Phys.* **2000**, *61*, 6138. (b) Boča, R. *Nova Biotechnol. Chim.* **2013**, *12*, 1.
(30) Bradley, C. J.; Cracknell, A. P. *The Mathematical Theory of Symmetry in Solids;* Clarendon Press: Oxford, U.K., 1972.
(31) Peng, Y.; Tian, C.-B.; Lan, Y.-H.; Magnani, N.; Li, Q.-P.; Zhang, H.-B.; Powell, A. K.; Du, S.-W. *Eur. J. Inorg. Chem.* **2013**, 5534.
(32) (a) Liu, Y.-H.; Tsai, H.-L.; Lu, Y.-L.; Wen, Y.-S.; Wang, J.-C.; Lu, K.-L. *Inorg. Chem.* **2001**, *40*, 6426. (b) Clemente-Juan, J. M.; Coronado, E.; Forment-Aliaga, A.; Galan-Mascaros, J. R.; Gimenez-Saiz, C.; Gomez-Garcia, C. J. *Inorg. Chem.* **2004**, *43*, 2689.